



Disruption of either the *Nfkb1* or the *Bcl3* gene inhibits skeletal muscle atrophy

R. Bridge Hunter and Susan C. Kandarian

Department of Health Sciences, Boston University, Boston, Massachusetts, USA.

The intracellular signals that mediate skeletal muscle protein loss and functional deficits due to muscular disuse are just beginning to be elucidated. Previously we showed that the activity of an NF-κB-dependent reporter gene was markedly increased in unloaded muscles, and p50 and Bcl-3 proteins were implicated in this induction. In the present study, mice with a knockout of the p105/p50 (*Nfkb1*) gene are shown to be resistant to the decrease in soleus fiber cross-sectional area that results from 10 days of hindlimb unloading. Furthermore, the marked unloading-induced activation of the NF-κB reporter gene in soleus muscles from WT mice was completely abolished in soleus muscles from *Nfkb1* knockout mice. Knockout of the B cell lymphoma 3 (*Bcl3*) gene also showed an inhibition of fiber atrophy and an abolition of NF-κB reporter activity. With unloading, fast fibers from WT mice atrophied to a greater extent than slow fibers. Resistance to atrophy in both strains of knockout mice was demonstrated clearly in fast fibers, while slow fibers from only the *Bcl3*^{-/-} mice showed atrophy inhibition. The slow-to-fast shift in myosin isoform expression due to unloading was also abolished in both *Nfkb1* and *Bcl3* knockout mice. Like the soleus muscles, plantaris muscles from *Nfkb1*^{-/-} and *Bcl3*^{-/-} mice also showed inhibition of atrophy with unloading. Thus both the *Nfkb1* and the *Bcl3* genes are necessary for unloading-induced atrophy and the associated phenotype transition.

Introduction

Reduced muscular activity due to bed rest, limb immobilization, sedentary lifestyles, or space flight is a widespread phenomenon that leads to significant muscle atrophy, weakness, fatigue, and insulin resistance (reviewed in ref. 1). While it has been known for some time that the loss in muscle protein due to disuse results from decreases in protein synthesis and increases in protein degradation rates (2), we are just beginning to learn about the upstream triggers and signaling pathways that regulate the changes in these target systems that determine protein content. While myostatin (3, 4) and glucocorticoids (5) have been studied for a role in atrophy, and both can induce atrophy in normal muscle, neither is required for disuse atrophy in vivo (5, 6). Recent work suggests that inhibition of the Akt growth pathway in muscle may be involved in the progression of disuse atrophy. Proteins of the Akt cascade of kinases involved in growth control are dephosphorylated with unloading (7–9). This is consistent with the decrease in protein synthesis rate.

Work from our laboratory has implicated additional regulatory molecules in unloading-induced muscle atrophy: the NF-κB and inhibitory κB (IκB) family of transcriptional regulators (10). We showed marked transactivation of injected NF-κB reporter plasmids in soleus muscles from non-weight-bearing (i.e., hindlimb-unloaded) rats. Gel-shift and immunoblot data using nuclear extracts of these muscles showed that likely NF-κB/IκB candidates for involvement in disuse atrophy were p50 and Bcl-3, but not p65. The canonical NF-κB pathway involves nuclear transport of a p65-p50 heterodimer as is seen with muscle atrophy due to cachexia (11, 12). Cytokines such as TNF-α are potent activators of the canonical NF-κB heterodimer, and this activation is associ-

ated with muscle protein loss (13, 14). However, in previous work, we did not find evidence for the involvement of TNF-α or inflammatory molecules with disuse, and this may explain the finding of a different, noncanonical NF-κB pathway in disuse atrophy (10).

Vertebrate NF-κB represents a family of 5 transcription factors (p65/RelA, c-Rel, RelB, p50, and p52) that contain a Rel homology domain, which confers the dimerization and DNA-binding properties. Active dimers of NF-κB can be formed by various combinations of family members (reviewed in refs. 15, 16). The IκB family members contain a conserved domain of 6–7 ankyrin repeats, which bind the Rel domain of NF-κB and prevent nuclear translocation. Activation of NF-κB occurs when IκBs are phosphorylated by the IκB kinase complex, leading to ubiquitination and degradation of IκB and nuclear translocation of the NF-κB dimer. Known IκBs include p105 and p100 (precursors to p50 and p52, respectively), IκBα, IκBβ, IκBγ, and IκBε (17).

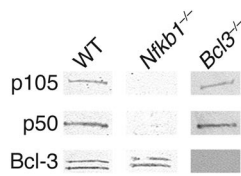
Another IκB family member, Bcl-3, is a protooncogene that is transcriptionally upregulated in some cases of chronic lymphocyte leukemia because of its location next to the breakpoint junction of a t(14;19) translocation. In various cancers, Bcl-3-p50 complexes have been shown to bind to NF-κB cis-elements and are thought to activate transcription (18–21). Generally, p50 and p52 homodimers, which lack transactivation domains, function as transcriptional repressors (22). However, upon binding with Bcl-3, these complexes can activate transcription through the Bcl-3 transactivation domain (23, 24). Thus, Bcl-3 is an unusual member of the IκB family, because it can function as a transcriptional coactivator.

As a direct extension of our previous work, here we tested whether the p105/p50 (*Nfkb1*) gene or the B cell lymphoma 3 (*Bcl3*) gene was required for unloading-induced NF-κB activation and muscle atrophy. To do this, we used knockout mice for each gene and determined NF-κB reporter activity, muscle fiber size, and general myosin phenotype after 10 days of hindlimb unloading. Compared with fiber atrophy of soleus muscles from WT mice, fiber atrophy of soleus muscles from both types of knock-

Nonstandard abbreviations used: *Bcl3*, B cell lymphoma 3; fMHC, fast myosin heavy chain; FOXO, forkhead box O; IκB, inhibitory κB.

Conflict of interest: The authors have declared that no conflict of interest exists.

Citation for this article: *J. Clin. Invest.* 114:1504–1511 (2004). doi:10.1172/JCI200421696.

**Figure 1**

Protein expression of p105, p50, and Bcl-3 from WT, *Nfkb1* knockout ($-/-$), and *Bcl3* knockout ($-/-$) mouse soleus muscle lysates by immunoblotting. There was no protein expression of Bcl-3 or of p105/p50 in extracts from the *Bcl3 $-/-$ or *Nfkb1 $-/-$ mice, respectively.**

out mice was abolished, while atrophy of the plantaris muscle was inhibited by 67% in these same mice. In the soleus, the sevenfold unloading-induced increase in WT NF- κ B reporter activity was eliminated in both strains of knockout mice. In knockout mice there also was a complete inhibition of the typical slow-to-fast shift in myosin isoform expression seen in WT mice. Overall, these data suggest that muscular inactivity triggers the activation of Bcl-3 and p50, which in turn may activate genes that are necessary for the induction of muscle atrophy.

Results

Descriptive characteristics of p105/p50 $-/-$ (Nfkb1 $-/-$) and Bcl3 $-/-$ mice. The mice lacking either the *Nfkb1* or the *Bcl3* gene were healthy, and there were no mobility or behavioral deficits. Body weights, muscle weights, and fiber number (counted in cross section) were similar in WT and knockout mice (not shown). Immunoblotting of soleus whole-muscle lysates showed no expression of p105/p50 or of Bcl-3 in extracts from the *Nfkb1 $-/-$ or *Bcl3 $-/-$ mice, respectively (Figure 1).**

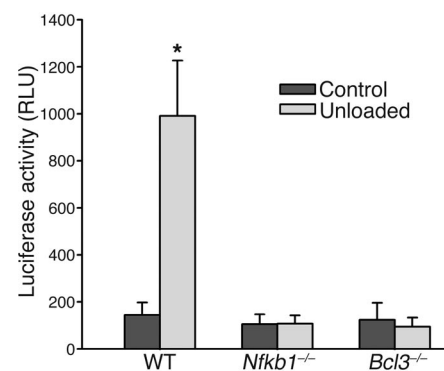
NF- κ B reporter activity in control and unloaded muscle from WT versus knockout mice. Recent work has shown that unloading of rat skeletal muscle leads to a marked increase in NF- κ B-dependent transcription, and p50 and Bcl-3 proteins were implicated in this activation (10). To investigate a potential role of p50 and Bcl-3 in this NF- κ B-dependent transactivation during disuse atrophy, we studied mice with a knockout of *Nfkb1* (which encodes the p105 and p50 protein) or *Bcl3*. To determine whether the NF- κ B-dependent reporter gene was activated in mice with unloading, the reporter plasmid was injected into soleus muscles, which were then assayed for luciferase. In WT mice, a sevenfold increase in luciferase activity was found after 10 days of unloading (Figure 2), similar to the activation observed in rats (10). However, there was no activation of the reporter in the *Nfkb1 $-/-$ or *Bcl3 $-/-$ mice after 10 days of unloading, which indicates that Bcl-3 and p50 are each required for NF- κ B-dependent reporter gene activation with muscle unloading.**

Muscle morphology and fiber size in control and unloaded muscle from WT versus knockout mice. The cross-sectional morphology of muscles was assessed using H&E stain, and these sections showed no evidence of degeneration, regeneration, or mononuclear infiltration in control or unloaded WT or knockout mice (Figure 3, A-F). Since p50 and Bcl-3 were required for activation of the NF- κ B reporter with unloading, we sought to determine whether they were required for the decrease in fiber size. Fiber cross-sectional area was used as a best measure of muscle atrophy to avoid potential confounding effects of extracellular space changes and so that the distribution of fiber sizes in the muscles could be assessed. Soleus muscle sections from WT, *Nfkb1 $-/-$, and *Bcl3 $-/-$ mice were**

stained for anti-laminin (Figure 3, G-L), and these sections were used to measure the fiber cross-sectional area. For experiments with mice, between 300 and 500 fibers were measured per muscle. The mean fiber size of the WT unloaded soleus muscles ($623 \pm 37 \mu\text{m}^2$) showed a 29% decrease (Figure 4A) compared with that of weight-bearing control muscles ($874 \pm 39 \mu\text{m}^2$). In the *Nfkb1 $-/-$ mice the soleus fiber atrophy was inhibited (control, $815 \pm 43 \mu\text{m}^2$; unloaded, $742 \pm 31 \mu\text{m}^2$). There was a similar inhibition of fiber atrophy in the *Bcl3 $-/-$ mice after unloading (control, $974 \pm 23 \mu\text{m}^2$; unloaded, $869 \pm 62 \mu\text{m}^2$). There were no statistically significant differences in control mean fiber area between WT and *Nfkb1 $-/-$ mice or between WT and *Bcl3 $-/-$ mice.****

Plotting the fiber areas as frequency distributions revealed a clear increase in the percentage of small fibers (i.e., a leftward shift) in the unloaded muscle of WT mice (Figure 4B). When the *Nfkb1* gene was knocked out, the shift to smaller fibers was inhibited (Figure 4C). The lack of *Bcl3* also inhibited the typical leftward shift of the fiber-size distribution (Figure 4D). The shape of the frequency distribution in the *Bcl3 $-/-$ mice was slightly different from that in either the WT or the *Nfkb1 $-/-$ mice. This mild effect on fiber-size distribution may be due to the absence of Bcl-3 protein during muscle development. Also, in some of the smaller-fiber-size categories in both knockout mice, there appear to be more fibers from unloaded than from control mice. This is likely a reflection of the 8% (in *Nfkb1 $-/-$ mice) and 11% (in *Bcl3 $-/-$ mice) difference in mean fiber area with unloading, which did not reach statistical significance.****

To determine whether the inhibition of atrophy occurred in another muscle besides the mixed (50% slow and 50% fast) soleus muscle, the fast plantaris muscle was also measured for changes in fiber size. Even though the mouse plantaris contains predominantly fast myosin (95% fast), it atrophied to an extent similar to that of the mouse soleus with unloading, as has also been shown by others (25–27). Plantaris muscle sections from WT, *Nfkb1 $-/-$, and *Bcl3 $-/-$ mice exhibited normal morphology based on the H&E stain (Figure 5, A-F). Sections stained for anti-laminin (immunofluorescence) were used to measure fiber cross-sectional area (Figure 5, G-L). The mean fiber size of the WT unloaded plantaris muscles ($789 \pm 53 \mu\text{m}^2$) was 27% smaller (Figure 6A) than that of weight-bearing control muscles**

**Figure 2**

NF- κ B reporter activity in control and unloaded muscle from WT versus knockout mice. WT mice showed a sevenfold activation of the NF- κ B-dependent reporter in unloaded ($n = 25$) compared with weight-bearing control muscles ($n = 24$). The NF- κ B-dependent activation seen in WT mice was eliminated in the *Nfkb1* (control, $n = 20$; unloaded, $n = 20$) and *Bcl3* (control, $n = 6$; unloaded, $n = 6$) knockout mice. *Mean value differs significantly from control ($P < 0.05$). RLU, relative luciferase units.

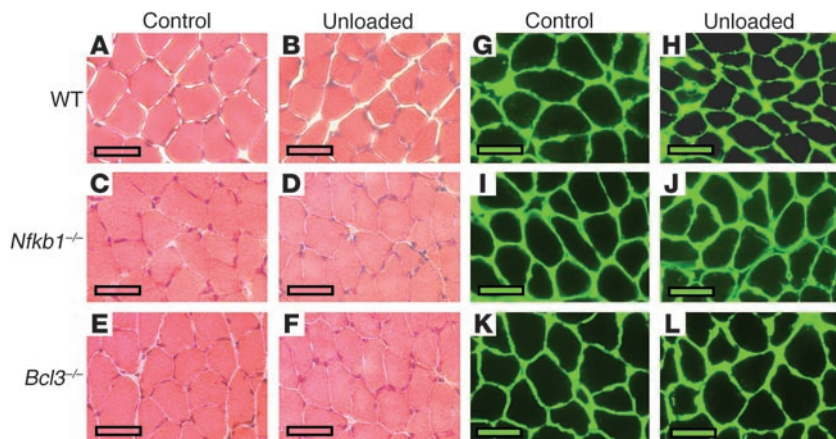


Figure 3 Soleus muscle cross sections in control and unloaded WT, *Nfkb1*^{-/-}, and *Bcl3*^{-/-} mice. (A–F) Morphology of representative sections using H&E stain. (G–L) Representative cross sections from anti-laminin–stained soleus muscles. The anti-laminin–stained sections were used for measurement of mean fiber area. Scale bars: 50 μm.

(1,087 ± 59 μm²). However, mean fiber area of *Nfkb1*^{-/-} mice only atrophied 9% due to unloading; this represents a 67% attenuation of atrophy (control, 958 ± 63 μm²; unloaded, 853 ± 40 μm²). Mean fiber area in the *Bcl3*^{-/-} mice only atrophied 10% because of unloading; this represents a 63% inhibition of atrophy (control, 954 ± 42 μm²; unloaded, 845 ± 62 μm²). To further describe the changes in fiber areas, frequency distributions were plotted. Fibers from unloaded WT mice showed a shift to a larger percentage of smaller fibers compared with fibers from the weight-bearing controls (Figure 6B). However, both the *Nfkb1*^{-/-} (Figure 6C) and the *Bcl3*^{-/-} (Figure 6D)

mice showed a much smaller difference in fiber-size distribution due to unloading compared with WT mice. The difference in the shapes of the frequency distributions between the soleus and the plantaris muscle is due to the differences in motor unit composition (28).

Myosin isoform expression in control and unloaded muscles from WT versus knockout mice. During muscle unloading it has long been noted that slow-twitch rodent muscles such as the soleus express more fast myosin isoforms and have faster shortening velocities than control muscles (reviewed in ref. 1). Since knockout of the *Nfkb1* and *Bcl3* genes largely inhibited atrophy, we also determined whether the absence of

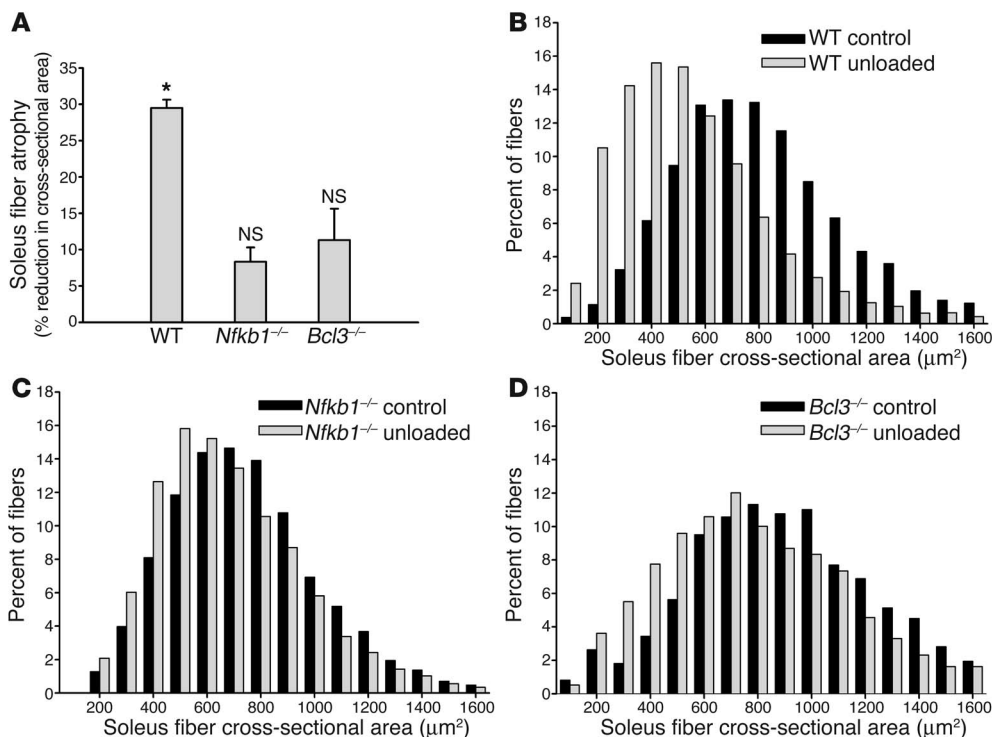


Figure 4 Fiber size in control and unloaded soleus muscles from WT versus knockout mice. (A) Mean percentage reduction in soleus fiber cross-sectional area in WT (control, *n* = 17 muscles; unloaded, *n* = 15 muscles), *Nfkb1*^{-/-} (control, *n* = 10 muscles; unloaded, *n* = 10 muscles), and *Bcl3*^{-/-} mice (control, *n* = 6 muscles; unloaded, *n* = 6 muscles) after 10 days of unloading. Mean fiber cross-sectional area decreased by 29% in WT mice and was not significantly different in control versus unloaded muscles of *Nfkb1*^{-/-} or *Bcl3*^{-/-} mice. (B–D) Frequency distribution of fiber cross-sectional area in control and unloaded WT (B), *Nfkb1*^{-/-} (C), and *Bcl3*^{-/-} mice (D). *Mean value differs significantly from control (*P* < 0.05).

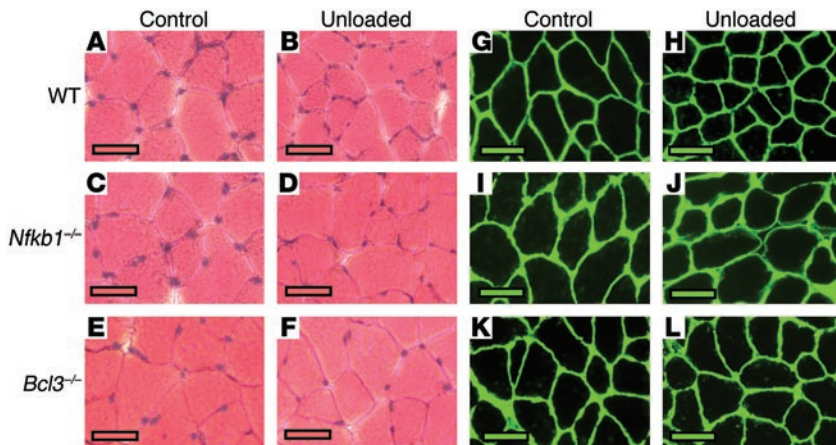


Figure 5 Plantaris muscle cross sections in control and unloaded WT, *Nfkb1*^{-/-}, and *Bcl3*^{-/-} mice. (A–F) Morphology of representative sections using H&E stain. (G–L) Representative cross sections from anti-laminin–stained plantaris muscles. The laminin sections were used for measurement of mean fiber area. Scale bars: 50 μm.

these genes would obviate the characteristic increase in fast myosin expression due to unloading. Muscle sections were immunostained using an antibody recognizing the fast myosin heavy chains (fMHCs) IIa and IIb (Figure 7, A–F). Unloaded WT mice exhibited a typical phenotypic shift to a faster muscle (Figure 7G). Expression of fMHC significantly increased by 12% in control compared with unloaded muscles. These results are consistent with recent reports of mice that underwent hindlimb unloading for 10 days (29) as well as other similar studies (reviewed in ref. 30). However, knockout of the *Nfkb1* gene completely abolished the shift to a faster muscle (Figure 7G). Similarly, in the *Bcl3*^{-/-} mice, the shift to a faster phenotype with unload-

ing was blocked. The phenotype of both knockout strains is slightly different from that of WT. Soleus muscles from *Nfkb1* knockout mice showed a 12% greater percentage of fibers expressing fMHC, while muscles from *Bcl3*^{-/-} mice expressed a 16% lower percentage of fMHC. However, independent of initial myosin isoform composition, the shift to a faster phenotype was abolished.

Atrophy of type I versus type II fibers in control and unloaded soleus muscles from WT versus knockout mice. The atrophy of the soleus muscle during hindlimb unloading is due to a decrease in fiber size with no change in fiber number (31). The decrease in cross-sectional area of type II (fast) fibers in the unloaded mouse soleus muscle is

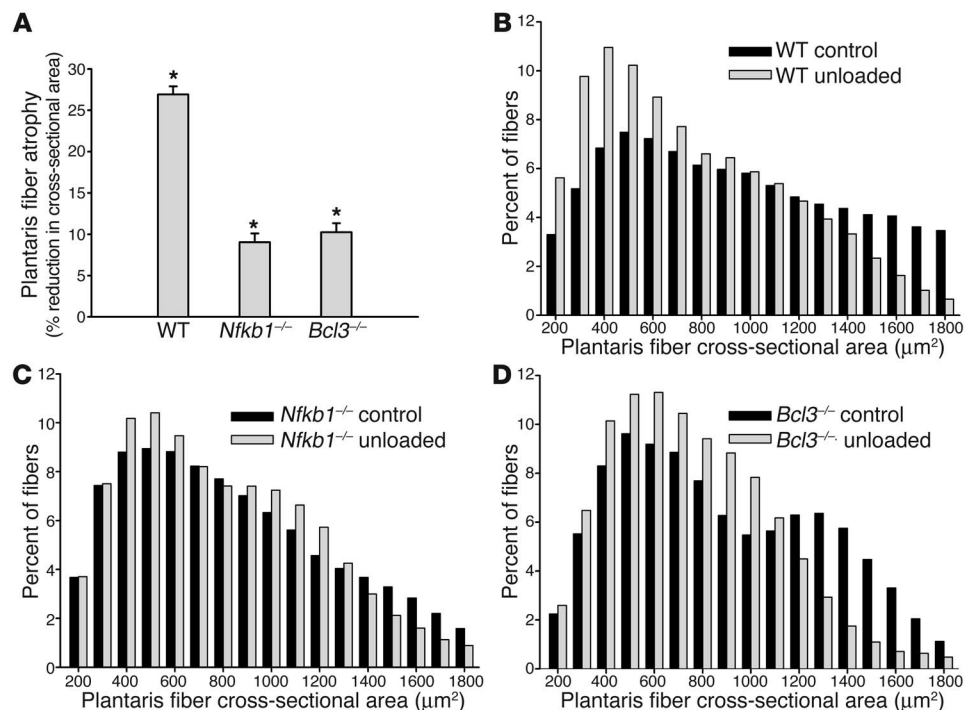


Figure 6 Fiber size in control and unloaded plantaris muscles from WT versus knockout mice. (A) Mean percentage reduction in plantaris fiber cross-sectional area in WT (control, *n* = 9 muscles; unloaded, *n* = 9 muscles), *Nfkb1*^{-/-} (control, *n* = 5 muscles; unloaded, *n* = 6 muscles), and *Bcl3*^{-/-} mice (control, *n* = 5 muscles; unloaded, *n* = 6 muscles) after 10 days of unloading. Mean fiber cross-sectional area decreased by 27%, 11%, and 11% in WT, *Nfkb1*^{-/-}, and *Bcl3*^{-/-} mice, respectively, after 10 days of unloading. (B–D) Frequency distribution of fiber cross-sectional area in control and unloaded WT (B), *Nfkb1*^{-/-} (C), and *Bcl3*^{-/-} mice (D). *Mean value differs significantly from control (*P* < 0.05).

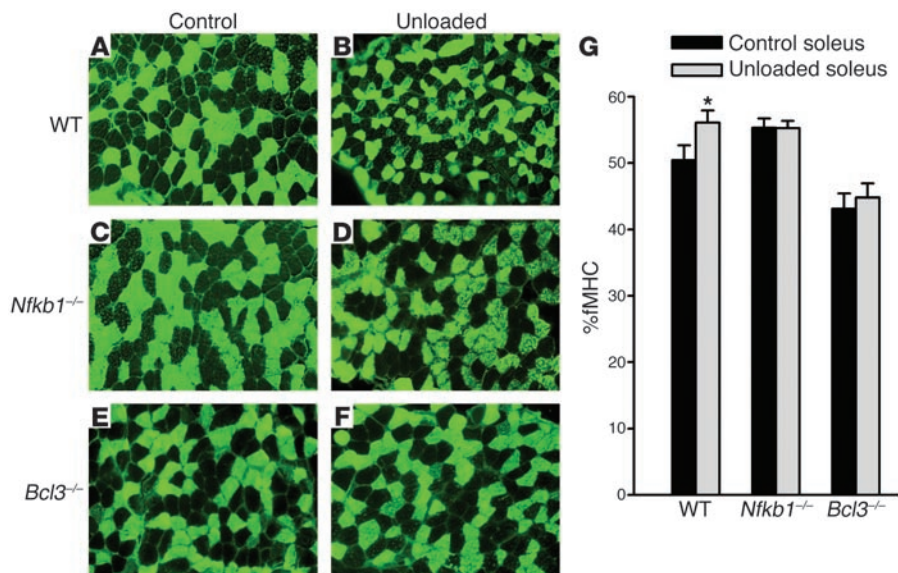


Figure 7

(A–F) Representative cross sections from anti-fMHC–stained soleus muscles from WT control ($n = 10$ muscles; **A**), WT unloaded ($n = 10$; **B**), *Nfkb1*^{-/-} control ($n = 7$; **C**), *Nfkb1*^{-/-} unloaded ($n = 7$; **D**), *Bcl3*^{-/-} control ($n = 6$; **E**), and *Bcl3*^{-/-} unloaded mice ($n = 6$; **F**). (**G**) Percentage of fibers in cross section that contain fMHC (i.e., IIb and IIa). Unloading significantly increased the percentage of fibers expressing fMHC in WT mice but not in *Nfkb1*^{-/-} and *Bcl3*^{-/-} mice. *Mean value differs significantly from control ($P < 0.05$).

equal to, and in some cases greater than, the atrophy seen in type I (slow) fibers within the first 2 weeks of the non-weight-bearing condition (reviewed in ref. 2). To determine whether there was a difference in atrophy in type I versus type II fibers due to unloading, we measured fiber type–specific cross-sectional area in WT mice. Fibers expressing fast myosin atrophied to a greater extent (33%) than slow fibers (17%) (Figure 8). To determine whether the inhibition of atrophy in the knockout mice was due to a lack of atrophy in slow and/or fast fibers, we assessed type I and type II fiber area in soleus muscles from *Nfkb1*^{-/-} and *Bcl3*^{-/-} mice. In *Nfkb1*^{-/-} mice, fast fibers atrophied only 10% and slow fibers atrophied 15%. Thus the inhibition of atrophy was marked in fast fibers, while atrophy occurred to a normal extent in slow fibers. In the *Bcl3*^{-/-} mice, there was a 12% decrease in fiber size in fast fibers and a lack of atrophy in slow fibers. The inhibition of atrophy in these mice was due to reduced atrophy in both fast and slow fibers.

While mouse soleus muscles have near-equal numbers of fast and slow fibers, fibers from plantaris muscles express predominantly (95%) fast myosin (data not shown). Thus the plantaris muscle atrophy seen with hindlimb unloading (27%) in WT mice (Figure 6A) can be attributed almost entirely to fast fibers. Thus the lack of atrophy in the plantaris muscles from *Nfkb1* and *Bcl3* knockout mice is due largely to the lack of atrophy of fast fibers.

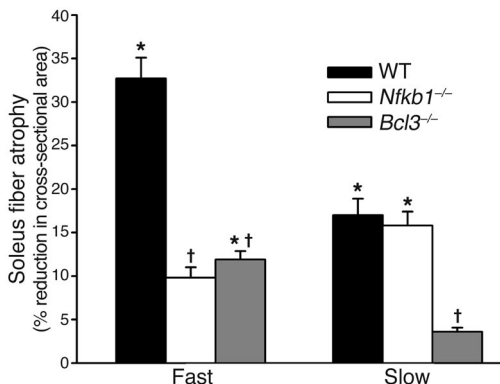
Figure 8

Fiber type–specific atrophy in control and unloaded soleus muscles from WT versus knockout mice. Mean percentage reduction in soleus cross-sectional area of slow and fast muscle fibers in WT (control, $n = 7$ muscles; unloaded, $n = 10$ muscles), *Nfkb1*^{-/-} (control, $n = 7$ muscles; unloaded, $n = 6$ muscles), and *Bcl3*^{-/-} mice (control, $n = 6$ muscles; unloaded, $n = 6$ muscles) after 10 days of unloading. Muscle fibers were classified as slow or fast on the basis of immunohistochemical staining with an anti-fMHC antibody. Fiber-size measurements were made from sections like those seen in Figure 7, A–F. *Unloaded mean value differs significantly from weight-bearing control ($P < 0.05$). †Knockout mean value differs significantly from WT ($P < 0.05$).

Discussion

This study establishes the requirement of 2 gene products for skeletal muscle atrophy due to disuse. Knockout of either of 2 members of the NF- κ B/I κ B family of transcriptional regulators, the *Nfkb1* gene and the *Bcl3* gene, not only abolished NF- κ B–dependent reporter activity but also inhibited the decreased fiber size due to disuse. The absence of either the *Nfkb1* or the *Bcl3* gene also abolished the shift from a mixed to a faster phenotype that is typically seen with unloading of WT animals. In WT mice, the fast fibers atrophied significantly more than the slow fibers. In *Nfkb1*^{-/-} mice, the inhibition of atrophy was due to a lack of atrophy in the fast fibers, while in *Bcl3*^{-/-} mice, there was an inhibition of atrophy in both the fast and the slow fibers.

The majority of work that has been performed on NF- κ B has involved the canonical p65-p50 heterodimer; however, our data support the requirement of Bcl-3 and p50 in muscle-disuse atrophy, because of the inhibition of NF- κ B activity and muscle fiber atrophy in mice with a knockout of either gene. Importantly, our previous work showed increased nuclear κ B–binding complexes containing Bcl-3 and p50, but not p65, in nuclear extracts from unloaded rat muscle (10). While p50 lacks a transactivation domain and homodimers can act as transcriptional repressors (22), Bcl-3–p50 complexes can activate transcription (24). Physiological examples





involving Bcl-3-p50 complexes have also been identified. Nasopharyngeal carcinoma is associated with Bcl-3-p50 complexes bound to the epithelial growth factor receptor promoter (18). Squamous cell carcinomas are associated with increased Bcl-3 expression and Bcl-3-p50 binding to κ B sites. In addition, overexpression of Bcl-3 in thymocytes (19) or in various B cell lines (20) leads to increased formation of nuclear Bcl-3-p50 complexes.

Several possible pathways lead to the formation of Bcl-3-p50 complexes in the nucleus. Increased Bcl-3 expression alone can lead to increased formation of Bcl-3-p50 complexes in thymocytes (19) and in B cell lines (20), without the processing of p105. Thus, it is possible that increased expression of Bcl-3 in unloaded muscle is driving the formation of Bcl-3-p50 complexes and that these are involved in the transactivation of specific κ B site-dependent genes. It is also possible that unloading induces the processing of p105. Inducible proteolysis of p105 by TNF, IL-1 β , or phorbol ester increases the formation of Bcl-3-p50 complexes, but p105 is completely processed; this implies the dimerization of newly released p50 proteins and either subsequent or concurrent sequestration by Bcl-3 (32). However, the upstream triggers for the involvement of Bcl-3 and p50 in the process of muscle-disuse atrophy have yet to be determined.

While the target genes of NF- κ B in muscle atrophy have not been elucidated, some downstream effects of NF- κ B activation include the induction of genes involved in the ubiquitin-proteasome pathway. Ubch2/E220k, a ubiquitin-conjugating gene involved in the ubiquitin-proteasome pathway, has been shown to be a target of NF- κ B in TNF- α -treated muscle cells (33). Our microarray data from control and unloaded rat muscle showed the upregulation of many genes involved in ubiquitin-proteasome-mediated degradation (34), and several of these genes have multiple NF- κ B sites in their regulatory regions, including the E3 (i.e., the ubiquitin-protein ligase) MAFbx/atrogen-1. While atrogen-1 was also activated in a cell culture condition where myotubes were fed only PBS for 6 hours, it did not show increased NF- κ B binding in a gel-shift assay (35). This suggests that PBS-fed ("starved") cells do not model the in vivo atrophy process that results from unloading. Nevertheless, genes involved in ubiquitination and proteasomal degradation may be NF- κ B targets during disuse atrophy, but this has yet to be determined experimentally.

Significant attention has been paid to the requirement of the ubiquitin-proteasome pathway for muscle atrophy (36). Much of this work focuses on the role of the ubiquitin ligases, in part because they have the greatest tissue and substrate specificity (37). Two groups simultaneously identified the muscle-specific F-box-containing ubiquitin-protein ligase MAFbx/atrogen-1 and found it to be markedly upregulated with atrophy due to disuse (38) and in cachexia (39). When MAFbx knockout mice are subjected to muscle denervation, gastrocnemius atrophy is attenuated by 56% at 14 days (38). Another E3 found to be increased by disuse atrophy (unloading, immobilization, or denervation) was a RING finger-containing ubiquitin ligase named MuRF1 (muscle RING finger 1). MuRF1 knockout mice showed a 36% attenuation of muscle atrophy after 14 days of gastrocnemius denervation (38).

Regarding other signaling pathways that may be involved in regulating atrophy, recent work implicates inhibition of the Akt growth pathway in the progression of disuse atrophy. The proteins of the Akt cascade of kinases involved in growth control have been shown to be dephosphorylated with unloading, consistent with the decreased protein synthesis rate. This includes Akt (7), mTOR

(8), and p70s6 kinase (7, 9), as well as the transcription initiation factor Phas-I (7). Overexpression of active Akt in denervated muscle prevents atrophy (7, 40), whereas inhibition of Akt produces mild atrophy in normal whole muscle and muscle cells (40, 41). When Akt is dephosphorylated, one of its targets, the forkhead box O (FOXO) family of transcription factors, is activated via dephosphorylation and then nuclear transport. This activity has been linked to the proteolysis associated with dexamethasone- and fasting-induced atrophy (35, 42). However, the requirement of FOXO during disuse atrophy is, at this time, only speculated (42).

A potential linkage between FOXO and NF- κ B signaling in muscle can be found in the literature. Muscle atrophy caused by immobilization (43) or unloading (44) is associated with oxidative stress and the generation of ROS. Components of the ubiquitin-proteasome system have been found to be transcriptional targets of ROS signaling in cultured myotubes (45, 46). Furthermore, ROS (via H₂O₂ treatment) induced activation of both the NF- κ B (47) and the FOXO signaling pathway (48) in muscle cells. In the case of NF- κ B, the signaling was associated with protein loss, and FOXO expression has been shown to decrease fiber size, via atrogen-1, in muscle (35). Therefore it appears possible that the increased ROS in unloading may trigger either the NF- κ B or the FOXO signaling pathway or both, perhaps leading to increased proteolysis through the ubiquitin-proteasome pathway, but this has yet to be directly tested.

A unique characteristic of muscle atrophy due to unloading (2, 29) and other disuse conditions (49-52) is the concomitant increase in fast myosin expression. This was reconfirmed in the present study in the WT unloaded soleus, but it was abolished in muscles of both *Nfkb1*^{-/-} and *Bcl3*^{-/-} mice. While the mechanism of the disuse-induced increase in fast myosin expression is not understood, there is evidence for a role of the transcriptional coactivator PGC-1 α (53) and the MEF2 family of transcription factors (reviewed in ref. 54) in the determination of muscle fiber type. Thus it is conceivable that knockout of either the p105/p50 or the Bcl3 gene could affect the genes involved in the regulation of the shift in fast myosin expression. Interestingly, Tidball and Spencer (29) also found no change in fast myosin expression in soleus muscles subjected to unloading for 10 days that were overexpressing calpastatin and that showed a 30% attenuation of atrophy. Thus, an alternative explanation for the lack of change in myosin expression with unloading where atrophy is also inhibited is that the regulation of atrophy and the change in myosin phenotype may be tightly linked.

Previously it has been shown that the decrease in cross-sectional area of type II (fast) fibers in the unloaded mouse soleus muscle is equal to, and in some cases greater than, the atrophy seen in the type I (slow) fibers within the first 2 weeks of the non-weight-bearing condition (reviewed in ref. 2). Results from the present study show that the extent of atrophy of slow fibers from WT mice was half that of the fast fibers. The inhibition of fiber atrophy in the *Nfkb1*^{-/-} mice was a result of the lack of atrophy of the fast fibers, while the slow fibers atrophied to the same extent in *Nfkb1*^{-/-} and WT mice (~16%). However, the inhibition of fiber atrophy in the *Bcl3*^{-/-} mice was due to a lack of atrophy of slow fibers and a significant reduction in the atrophy of fast fibers (Figure 8). While mice lacking either the *Nfkb1* or the *Bcl3* gene show inhibited muscle atrophy, there may be differences in the way each gene regulates atrophy. Given the slight difference in myosin phenotype and the slight difference in slow and fast fiber atrophy in the 2 types of knockout mice, it would not be surprising if there were somewhat different regulatory mechanisms of muscle atrophy in the *Nfkb1*^{-/-} versus the *Bcl3*^{-/-} mice.



In summary, the results of this study demonstrate that knockout of the *Nfkb1* or the *Bcl3* gene inhibits muscle atrophy, phenotype change, and activation of NF- κ B activity due to hindlimb-unloading disuse. Atrophy was inhibited in both a mixed mouse muscle (the soleus, 50% fast myosin) and a predominantly fast muscle (the plantaris, 95% fast myosin). Taken together, these results demonstrate the requirement of NF- κ B signaling in disuse muscle atrophy and the associated phenotype change. Further work is needed to elucidate the upstream triggers of this signaling and the downstream genes targeted by NF- κ B.

Methods

Animals and hindlimb unloading. Normal 8-week-old female B6;129, Nfkb1-deficient (*Nfkb1*^{-/-}) B6;129, and Bcl-3-deficient (*Bcl3*^{-/-}) B6;129 mice were purchased from The Jackson Laboratory. All mice were housed in the Boston University Animal Care Facilities under pathogen-free conditions. The mice were randomly assigned to control or hindlimb-unloaded groups. To induce muscle atrophy by disuse (i.e., reduced muscle tension), the rodent’s hindlimbs were suspended off the cage floor (by 1 mm) using elastic tail casts, as described previously (55), for 10 days. The use of animals in this study was approved by the Boston University Institutional Animal Care and Use Committee.

Muscle preparation and analysis. At the end of the experimental treatments, control and unloaded mice were anesthetized with ketamine/xylazine (100 mg/kg), and soleus muscles from right and left hindlimbs were removed, quickly weighed, and either processed immediately for protein assays (see below) or embedded in tissue-freezing medium and frozen in isopentane for sectioning and subsequent morphological and immunohistochemical analysis.

Somatic gene transfer using intramuscular DNA injection. NF- κ B-GL3 contains a trimerized NF- κ B site from the Igk light chain enhancer. These sequences, gifts from S. Ho (UCSD, San Diego, California, USA), were each inserted into the IL-2 minimal promoter (56) driving expression of luciferase in pGL3-basic. Plasmid DNA injections into skeletal muscle have been previously detailed (57). Plasmid DNA was prepared using an EndoFree Plasmid Mega Kit (QIAGEN Inc.). The DNA was ethanol-precipitated and then resuspended at 4°C overnight in 1x PBS. Prior to plasmid injection, control and unloaded animals were anesthetized with ketamine/xylazine (100 mg/kg). Mouse soleus muscles were injected with 10 μ g plasmid DNA in a volume of 5 μ l. Eleven days after injection, muscles were removed for analysis of luciferase activity. Hindlimb unloading does not influence the efficiency of plasmid DNA uptake compared with that in weight-bearing control muscles (57). Control and unloaded muscles were ground with a tissue homogenizer in 100 μ l of passive lysis buffer (Promega Corp.). Homogenates were centrifuged at 5,500 g for 20 minutes at 4°C. Twenty microliters of the supernatant was used to determine firefly luciferase activity using a luciferase assay kit (Promega Corp.) and a Turner Designs Inc. luminometer (model TD-20/20). Activity values reflect total muscle luciferase activity.

Western blot analysis. Muscle lysates were prepared by grinding with a tissue homogenizer in passive lysis buffer (Promega Corp.) and centrifuging at 5,500 g for 20 minutes at 4°C, and the resultant supernatant was used as lysate. Twenty micrograms of protein from soleus muscle lysates was

denatured in SDS loading buffer, boiled for 3 minutes, centrifuged briefly to remove insoluble material, and separated on SDS-polyacrylamide gels. Protein was transferred onto Hybond ECL (Amersham Biosciences) nitrocellulose membrane. Membranes were blocked in 5% nonfat milk diluted in TBS-Tween for 1 hour and then incubated for 1–2 hours with the appropriate antibody diluted according to the manufacturer’s instructions. HRP-conjugated secondary antibodies and a chemiluminescent detection system (Amersham Biosciences) were used for visualization. The Bcl-3 (sc-185) antibody used for immunoblotting was obtained from Santa Cruz Biotechnology Inc. The p105/p50 (ab7549) antibody was purchased from Novus Biologicals Inc. Secondary antibodies (HRP-labeled goat anti-rabbit) were obtained from Transduction Laboratories.

Histochemistry. Muscles frozen in isopentane were sectioned (10 μ m) from the midbelly and fixed in 1.5% formalin. Sections were then stained with hematoxylin for 30 seconds and then with eosin for 60 seconds. Images were visualized using a light microscope (Nikon Inc.) and captured with a SPOT RT camera and SPOT software (Diagnostic Instruments Inc.).

Immunohistochemical analysis. Muscles frozen in isopentane were sectioned (10 μ m) from the midbelly and fixed in 4% paraformaldehyde. For measurement of fiber size, sections were then blocked in 10% BSA in PBS for 1 hour, then incubated in anti-laminin (L9393; Sigma-Aldrich) overnight at room temperature. Alexa Fluor 488 (Invitrogen Corp.) fluorescent dye conjugated to an anti-rabbit secondary antibody was used for visualization. Images were visualized with a fluorescence microscope (Nikon Inc.) and captured with a SPOT RT camera and SPOT software (Diagnostic Instruments Inc.), and fiber cross-sectional area measurements were calculated using the MetaMorph Imaging System (Universal Imaging Corp.).

To determine fiber type, 10- μ m sections were fixed in 4% paraformaldehyde and rinsed, and then the endogenous IgG was blocked using a Mouse on Mouse (M.O.M.) kit (Vector Laboratories Inc.). Sections were blocked with 10% BSA and then incubated with a mouse mAb that recognizes both IIa and IIb fMHCs (clone WB-MHCf; Novocastra Laboratories Ltd.). Alexa Fluor 488 (Invitrogen Corp.) fluorescent dye conjugated to an anti-mouse secondary antibody was used for visualization.

Statistics. For fiber cross-sectional area, luciferase activity, and fiber type, a Student’s *t* test for unpaired data was used to determine statistical significance between control and unloaded groups at *P* < 0.05. The number of muscles studied for each experiment is given in the figure legends.

Acknowledgments

This work was supported by the National Space Biomedical Research Institute (NSBRI MA00207) and by the National Institute of Arthritis and Musculoskeletal and Skin Diseases (R01 AR41705). We thank Paul Giresi and Alan Koncarevic for technical assistance and Robert Jackman for editorial comments.

Received for publication March 24, 2004, and accepted in revised form September 21, 2004.

Address correspondence to: Susan C. Kandarian, Department of Health Sciences, Boston University, 635 Commonwealth Avenue, Room 443, Boston, Massachusetts 02215, USA. Phone: (617) 353-5169; Fax: (617) 353-7567; E-mail: skandar@bu.edu.

1. Booth, F., and Baldwin, K. 1996. Muscle plasticity: energy demand/supply processes. In *Exercise: regulation and integration of multiple systems*. L. Rowell and J. Sheperd, editors. Published for the American Physiological Society. Oxford University Press. New York, New York, USA. 1075–1123.
 2. Thomason, D.B., and Booth, F.W. 1990. Atrophy of the soleus muscle by hindlimb unweighting.

J. Appl. Physiol. **68**:1–12.
 3. Zimmers, T.A., et al. 2002. Induction of cachexia in mice by systemically administered myostatin. *Science*. **296**:1486–1488.
 4. Sharma, M., Langley, B., Bass, J., and Kambadur, R. 2001. Myostatin in muscle growth and repair. *Exerc. Sport Sci. Rev.* **29**:155–158.
 5. Tischler, M.E. 1994. Effect of the antigluco-

coid RU38486 on protein metabolism in unweighted soleus muscle. *Metabolism*. **43**:1451–1455.
 6. McMahon, C.D., et al. 2003. Myostatin-deficient mice lose more skeletal muscle mass than wild-type controls during hindlimb suspension. *Am. J. Physiol. Endocrinol. Metab.* **285**:E82–E87.
 7. Bodine, S.C., et al. 2001. Akt/mTOR pathway is a crucial regulator of skeletal muscle hypertrophy



- and can prevent muscle atrophy in vivo. *Nat. Cell Biol.* **3**:1014–1019.
8. Reynolds, T.H., 4th, Bodine, S.C., and Lawrence, J.C., Jr. 2002. Control of Ser2448 phosphorylation in the mammalian target of rapamycin by insulin and skeletal muscle load. *J. Biol. Chem.* **277**:17657–17662.
9. Hornberger, T.A., Hunter, R.B., Kandarian, S.C., and Esser, K.A. 2001. Regulation of translation factors during hindlimb unloading and denervation of skeletal muscle in rats. *Am. J. Physiol. Cell Physiol.* **281**:C179–C187.
10. Hunter, R.B., et al. 2002. Activation of an alternative NF-kappaB pathway in skeletal muscle during disuse atrophy. *FASEB J.* **16**:529–538.
11. Mitch, W.E., and Price, S.R. 2001. Transcription factors and muscle cachexia: is there a therapeutic target? *Lancet.* **357**:734–735.
12. Hasselgren, P.O., and Fischer, J.E. 2001. Muscle cachexia: current concepts of intracellular mechanisms and molecular regulation. *Ann. Surg.* **233**:9–17.
13. Guttridge, D.C., Mayo, M.W., Madrid, L.V., Wang, C.Y., and Baldwin, A.S., Jr. 2000. NF-kappaB-induced loss of MyoD messenger RNA: possible role in muscle decay and cachexia. *Science.* **289**:2363–2366.
14. Li, Y.P., and Reid, M.B. 2000. NF-kappaB mediates the protein loss induced by TNF-alpha in differentiated skeletal muscle myotubes. *Am. J. Physiol. Regul. Integr. Comp. Physiol.* **279**:R1165–R1170.
15. Senfiteben, U., and Karin, M. 2002. The IKK/NF-kappaB pathway. *Crit. Care Med.* **30**(Suppl. 1):S18–S26.
16. Ghosh, S., May, M.J., and Kopp, E.B. 1998. NF-kappaB and Rel proteins: evolutionarily conserved mediators of immune responses. *Annu. Rev. Immunol.* **16**:225–260.
17. Yamamoto, Y., and Gaynor, R.B. 2004. IkkappaB kinases: key regulators of the NF-kappaB pathway. *Trends Biochem. Sci.* **29**:72–79.
18. Thornburg, N.J., Pathmanathan, R., and Raab-Traub, N. 2003. Activation of nuclear factor-kappaB p50 homodimer/Bcl-3 complexes in nasopharyngeal carcinoma. *Cancer Res.* **63**:8293–8301.
19. Caamano, J.H., Perez, P., Lira, S.A., and Bravo, R. 1996. Constitutive expression of Bcl-3 in thymocytes increases the DNA binding of NF-kappaB1 (p50) homodimers in vivo. *Mol. Cell. Biol.* **16**:1342–1348.
20. Watanabe, N., Iwamura, T., Shinoda, T., and Fujita, T. 1997. Regulation of NFkB1 proteins by the candidate oncoprotein Bcl-3: generation of NF-kappaB homodimers from the cytoplasmic pool of p50-p105 and nuclear translocation. *EMBO J.* **16**:3609–3620.
21. Dechend, R., et al. 1999. The Bcl-3 oncoprotein acts as a bridging factor between NF-kappaB/Rel and nuclear co-regulators. *Oncogene.* **18**:3316–3323.
22. Franzoso, G., et al. 1992. The candidate oncoprotein Bcl-3 is an antagonist of p50/NF-kappaB-mediated inhibition. *Nature.* **359**:339–342.
23. Bours, V., et al. 1993. The oncoprotein Bcl-3 directly transactivates through kappaB motifs via association with DNA-binding p50B homodimers. *Cell.* **72**:729–739.
24. Fujita, T., Nolan, G.P., Liou, H.C., Scott, M.L., and Baltimore, D. 1993. The candidate proto-oncogene bcl-3 encodes a transcriptional coactivator that activates through NF-kappa B p50 homodimers. *Genes Dev.* **7**:1354–1363.
25. Vandenberg, H., et al. 1998. Attenuation of skeletal muscle wasting with recombinant human growth hormone secreted from a tissue-engineered bioartificial muscle. *Hum. Gene Ther.* **9**:2555–2564.
26. Kasper, C.E., and Xun, L. 1996. Cytoplasm-to-myonucleus ratios in plantaris and soleus muscle fibres following hindlimb suspension. *J. Muscle Res. Cell Motil.* **17**:603–610.
27. Mitchell, P.O., and Pavlath, G.K. 2001. A muscle precursor cell-dependent pathway contributes to muscle growth after atrophy. *Am. J. Physiol. Cell Physiol.* **281**:C1706–C1715.
28. Saltin, B., and Gollnick, P.D. 1983. Skeletal muscle adaptability: significance for metabolism and performance. In *Skeletal muscle*. R.H. Adrian, editor. American Physiological Society. Bethesda, Maryland, USA. 555–631.
29. Tidball, J.G., and Spencer, M.J. 2002. Expression of a calpastatin transgene slows muscle wasting and obviates changes in myosin isoform expression during murine muscle disuse. *J. Physiol.* **545**:819–828.
30. Pette, D., and Staron, R.S. 2001. Transitions of muscle fiber phenotypic profiles. *Histochem. Cell Biol.* **115**:359–372.
31. Templeton, G.H., Sweeney, H.L., Timson, B.F., Padalino, M., and Dudenhoefter, G.A. 1988. Changes in fiber composition of soleus muscle during rat hindlimb suspension. *J. Appl. Physiol.* **65**:1191–1195.
32. Heissmeyer, V., Krappmann, D., Wulczyn, F.G., and Scheidereit, C. 1999. NF-kappaB p105 is a target of IkkappaB kinases and controls signal induction of Bcl-3-p50 complexes. *EMBO J.* **18**:4766–4778.
33. Li, Y.P., et al. 2003. TNF-alpha increases ubiquitin-conjugating activity in skeletal muscle by up-regulating UbH2c/E220k. *FASEB J.* **17**:1048–1057.
34. Stevenson, E.J., Giresi, P.G., Koncarevic, A., and Kandarian, S.C. 2003. Global analysis of gene expression patterns during disuse atrophy in rat skeletal muscle. *J. Physiol.* **551**:33–48.
35. Sandri, M., et al. 2004. Foxo transcription factors induce the atrophy-related ubiquitin ligase atrogen-1 and cause skeletal muscle atrophy. *Cell.* **117**:399–412.
36. Lecker, S.H. 2003. Ubiquitin-protein ligases in muscle wasting: multiple parallel pathways? *Curr. Opin. Clin. Nutr. Metab. Care.* **6**:271–275.
37. Hershko, A., and Ciechanover, A. 1998. The ubiquitin system. *Annu. Rev. Biochem.* **67**:425–479.
38. Bodine, S.C., et al. 2001. Identification of ubiquitin ligases required for skeletal muscle atrophy. *Science.* **294**:1704–1708.
39. Gomes, M.D., Lecker, S.H., Jagoe, R.T., Navon, A., and Goldberg, A.L. 2001. Atrogen-1, a muscle-specific F-box protein highly expressed during muscle atrophy. *Proc. Natl. Acad. Sci. U. S. A.* **98**:14440–14445.
40. Pallafacchina, G., Calabria, E., Serrano, A.L., Kalhovde, J.M., and Schiaffino, S. 2002. A protein kinase B-dependent and rapamycin-sensitive pathway controls skeletal muscle growth but not fiber type specification. *Proc. Natl. Acad. Sci. U. S. A.* **99**:9213–9218.
41. Rommel, C., et al. 2001. Mediation of IGF-1-induced skeletal myotube hypertrophy by PI(3)K/Akt/mTOR and PI(3)K/Akt/GSK3 pathways. *Nat. Cell Biol.* **3**:1009–1013.
42. Stitt, T.N., et al. 2004. The IGF-1/PI3K/Akt pathway prevents expression of muscle atrophy-induced ubiquitin ligases by inhibiting FOXO transcription factors. *Mol. Cell.* **14**:395–403.
43. Kondo, H., Miura, M., and Ito, Y. 1991. Oxidative stress in skeletal muscle atrophied by immobilization. *Acta Physiol. Scand.* **142**:527–528.
44. Lawler, J.M., Song, W., and Demaree, S.R. 2003. Hindlimb unloading increases oxidative stress and disrupts antioxidant capacity in skeletal muscle. *Free Radic. Biol. Med.* **35**:9–16.
45. Gomes-Marcondes, M.C., and Tisdale, M.J. 2002. Induction of protein catabolism and the ubiquitin-proteasome pathway by mild oxidative stress. *Cancer Lett.* **180**:69–74.
46. Li, Y.P., Chen, Y., Li, A.S., and Reid, M.B. 2003. Hydrogen peroxide stimulates ubiquitin-conjugating activity and expression of genes for specific E2 and E3 proteins in skeletal muscle myotubes. *Am. J. Physiol. Cell Physiol.* **285**:C806–C812.
47. Li, Y.P., Schwartz, R.J., Waddell, I.D., Holloway, B.R., and Reid, M.B. 1998. Skeletal muscle myocytes undergo protein loss and reactive oxygen-mediated NF-kappaB activation in response to tumor necrosis factor alpha. *FASEB J.* **12**:871–880.
48. Furukawa-Hibi, Y., Yoshida-Araki, K., Ohta, T., Ikeda, K., and Motoyama, N. 2002. FOXO forkhead transcription factors induce G(2)-M checkpoint in response to oxidative stress. *J. Biol. Chem.* **277**:26729–26732.
49. Jankala, H., Harjola, V.P., Petersen, N.E., and Harkonen, M. 1997. Myosin heavy chain mRNA transform to faster isoforms in immobilized skeletal muscle: a quantitative PCR study. *J. Appl. Physiol.* **82**:977–982.
50. Dupont-Versteegden, E.E., Knox, M., Gurley, C.M., Houle, J.D., and Peterson, C.A. 2002. Maintenance of muscle mass is not dependent on the calcineurin-NFAT pathway. *Am. J. Physiol. Cell Physiol.* **282**:C1387–C1395.
51. Caiozzo, V.J., Haddad, F., Baker, M.J., and Baldwin, K.M. 1995. Functional and cellular adaptations of rodent skeletal muscle to weightlessness. *J. Gravit. Physiol.* **2**:P39–P42.
52. Widrick, J.J., et al. 1997. Effect of 17 days of bed rest on peak isometric force and unloaded shortening velocity of human soleus fibers. *Am. J. Physiol.* **273**:C1690–C1699.
53. Lin, J., et al. 2002. Transcriptional co-activator PGC-1 alpha drives the formation of slow-twitch muscle fibres. *Nature.* **418**:797–801.
54. Olson, E.N., and Williams, R.S. 2000. Remodeling muscles with calcineurin. *Bioessays.* **22**:510–519.
55. Peters, D.G., Mitchell-Felton, H., and Kandarian, S.C. 1999. Unloading induces transcriptional activation of the sarco(endo)plasmic reticulum Ca2+-ATPase 1 gene in muscle. *Am. J. Physiol.* **276**:C1218–C1225.
56. Durand, D.B., et al. 1988. Characterization of antigen receptor response elements within the interleukin-2 enhancer. *Mol. Cell. Biol.* **8**:1715–1724.
57. Mitchell-Felton, H., and Kandarian, S.C. 1999. Normalization of muscle plasmid uptake by Southern blot: application to SERCA1 promoter analysis. *Am. J. Physiol.* **277**:C1269–C1276.